


# T cell infiltration on local CpG-B delivery in early-stage melanoma is predominantly related to CLEC9A<sup>+</sup>CD141<sup>+</sup> cDC1 and CD14<sup>+</sup> antigen-presenting cell recruitment

Bas D Koster,<sup>1</sup> Marta López González ,<sup>1</sup> Mari FCM van den Hout,<sup>1,2</sup> Annelies W Turksma,<sup>2</sup> Berbel JR Sluijter,<sup>3</sup> Barbara G Molenkamp,<sup>3</sup> Paul AM van Leeuwen,<sup>3</sup> Saskia Vosslamber,<sup>2</sup> Rik J Scheper,<sup>2</sup> Alfons JM van den Eertwegh,<sup>1</sup> M Petrousjka van den Tol,<sup>3</sup> Ekaterina J Jordanova,<sup>1,4</sup> Tanja D de Gruijl<sup>1</sup>

**To cite:** Koster BD, López González M, van den Hout MFCM, *et al.* T cell infiltration on local CpG-B delivery in early-stage melanoma is predominantly related to CLEC9A<sup>+</sup>CD141<sup>+</sup> cDC1 and CD14<sup>+</sup> antigen-presenting cell recruitment. *Journal for ImmunoTherapy of Cancer* 2021;**9**:e001962. doi:10.1136/jitc-2020-001962

► Additional material is published online only. To view, please visit the journal online (<http://dx.doi.org/10.1136/jitc-2020-001962>).

BDK and MLG contributed equally.

Accepted 10 February 2021



© Author(s) (or their employer(s)) 2021. Re-use permitted under CC BY-NC. No commercial re-use. See rights and permissions. Published by BMJ.

For numbered affiliations see end of article.

## Correspondence to

Professor Tanja D de Gruijl; [td.degruijl@amsterdamumc.nl](mailto:td.degruijl@amsterdamumc.nl)

## ABSTRACT

**Background** We previously reported CpG-B injection at the primary tumor excision site prior to re-excision and sentinel node biopsy to result in immune activation of the sentinel lymph node (SLN), increased melanoma-specific CD8<sup>+</sup> T cell rates in peripheral blood, and prolonged recurrence-free survival. Here, we assessed recruitment and activation of antigen-presenting cell (APC) subsets in the SLN and at the injection site in relation to T cell infiltration.

**Methods** Re-excision skin specimens from patients with clinical stage I-II melanoma, collected 7 days after intradermal injection of either saline (n=10) or 8 mg CpG-B (CPG7909, n=12), were examined by immunohistochemistry, quantifying immune subsets in the epidermis, papillary, and reticular dermis. Counts were related to flow cytometric data from matched SLN samples. Additional *in vitro* cultures and transcriptional analyses on peripheral blood mononuclear cells (PBMCs) were performed to ascertain CpG-induced APC activation and chemokine profiles.

**Results** Significant increases in CD83<sup>+</sup>, CD14<sup>+</sup>, CD68<sup>+</sup>, and CD123<sup>+</sup> APC were observed in the reticular dermis of CpG-B-injected skin samples. Fluorescent double/triple staining revealed recruitment of both CD123<sup>+</sup>BDCA2<sup>+</sup> plasmacytoid dendritic cells (DCs) and BDCA3/CD141<sup>+</sup>CLEC9A<sup>+</sup> type-1 conventional DC (cDC1), of which only the cDC1 showed considerable levels of CD83 expression. Simultaneous CpG-B-induced increases in T cell infiltration were strongly correlated with both cDC1 and CD14 counts. Moreover, cDC1 and CD14<sup>+</sup> APC rates in the reticular dermis and matched SLN suspensions were positively correlated. Flow cytometric, transcriptional, and chemokine release analyses of PBMC, *in vitro* or *in vivo* exposure to CpG-B, indicate a role for the activation and recruitment of both cDC1 and CD14<sup>+</sup> monocyte-derived APCs in the release of CXCL10 and subsequent T cell infiltration.

**Conclusion** The CpG-B-induced concerted recruitment of cDC1 and CD14<sup>+</sup> APC to the injection site and its draining

lymph nodes may allow for both the (cross-)priming of T cells and their subsequent homing to effector sites.

## INTRODUCTION

Conventional dendritic cells (cDCs) in the healthy skin are capable of capturing and processing antigens before migrating to the regional lymph nodes where they can elicit an immune response by stimulating antigen-specific T cells.<sup>1</sup> Langerhans cells (LCs), with high expression levels of CD1a and Langerin, are mainly found in the epidermis, whereas CD1a<sup>+</sup>CD1c<sup>+</sup> dermal DC, which may or may not coexpress CD14,<sup>2</sup> are found in the dermis of healthy steady-state skin. A third, low-frequency skin cDC subset, also found in the dermis, is the BDCA3/CD141<sup>+</sup> DC population. This subset, designated as cDC1, is superior at cross-presenting antigens and expresses relatively high levels of the C-type lectin receptor CLEC9A.<sup>3</sup> Besides cDC, a CD14<sup>+</sup> macrophage-like APC subset represents a large part of the APC that are found in healthy skin.<sup>1</sup> Compared with cDC, these macrophage-like cells have a rapid turnover and poor antigen presenting and migrating capabilities, but serve a role in the boosting and maintenance of (tissue-resident) memory T cells.<sup>4</sup> In inflamed skin, another class of DC called plasmacytoid dendritic cells (pDCs) can be found.<sup>5</sup> Even though these are relatively weak T effector cell primers,<sup>6</sup> pDCs elicit a powerful immune response by producing large amounts of type-I interferons (IFN-I), like IFN $\alpha$  and IFN $\beta$ , on activation, which in turn can activate cDC, CD8<sup>+</sup> effector T cells,

and Natural Killer (NK) cells. In addition, inflammation can lead to the recruitment and local differentiation of monocyte-derived APC subsets.

In patients with melanoma, DC development and activation is hampered in the tumor microenvironment (TME) due to the local release of soluble mediators such as interleukin (IL)-10, prostaglandins, Vascular Endothelial Growth Factor (VEGF), IL-6, and Transforming Growth Factor (TGF)- $\beta$ .<sup>7</sup> We recently also demonstrated a role for hampered DC activation in the first-line melanoma-draining lymph node, the so-called sentinel lymph node (SLN) in early immune escape.<sup>8</sup> This inhibited DC development and activation not only hampers T cell priming but also blocks effector T cell recruitment to the TME, thus effectively interfering with the efficacy of both immune checkpoint blockade and (in vivo) vaccination approaches. DC express Toll-like receptors (TLRs) that can recognize molecular patterns from pathogens, leading to their activation. TLR-L have been clinically explored, both as vaccine adjuvants and as intratumorally applied immune modulators, aiming at DC recruitment and activation in the TME, thus ameliorating tumor-related immune suppression and facilitating effector T cell (cross-)priming and recruitment. Unlike cDC, human pDC express TLR9 that binds unmethylated cytosine-phosphate-guanine (CpG) oligodeoxynucleotides (ODN).<sup>9</sup> CPG7909 (CpG-B 2006/PF-3512676) is a synthetic B-class CpG ODN (hereafter simply referred to as CpG-B) with a full phosphorothioate backbone with multiple unmethylated CpG dinucleotides. It strongly activates B cells and TLR9-dependent NF- $\kappa$ B signaling and can stimulate type-I IFN secretion.<sup>10 11</sup> We previously reported on two phase II clinical trials, in which patients with clinical stage I-II melanoma received intradermal injections with either CpG-B/CPG7909 or plain saline in the week leading up to a sentinel node biopsy (SNB) and a re-excision of the primary tumor excision scar. We found that this local intradermal administration of CpG-B resulted in activation of both lymph node resident (LNR-) cDC and pDC subsets in the SLN,<sup>12</sup> elevated frequencies of tumor-specific T cells in the peripheral blood,<sup>13</sup> lower rates of tumor-positive SLN, and even an increased recurrence-free survival, as compared with the administration of a saline placebo in the control group.<sup>14</sup>

Here, we set out to study the local effects of intradermal CpG-B injection at the primary tumor re-excision site in terms of APC subset recruitment and activation. We related our findings to DC subset content of matched SLN samples as well as to T cell infiltration, in order to gain further insight in the locoregional events leading up to T cell activation and recruitment, and, eventually, to systemic tumor control.

## MATERIALS AND METHODS

### Patients

This study made use of clinical materials and immune monitoring data collected over the course of two

consecutive single-center, single-blinded, randomized, and placebo-controlled phase II clinical trials, conducted between June 2004 and June 2007 at the VU University Medical Center in Amsterdam, The Netherlands (ISRCTN63321797). Enrolled patients were diagnosed with clinical stage I-II melanoma according to criteria of the American Joint Committee on Cancer and were scheduled to undergo SNB. Patients who had undergone previous immunotherapy or chemotherapy were excluded as well as patients receiving immunosuppressive medication or suffering from any autoimmune disorder. They were randomly assigned to receive preoperative local administration of either CpG-B (PF-3512676; Coley Pharmaceutical Group, Wellesley, Massachusetts, USA) or saline (NaCl 0.9%) adjacent to the excision scar of the primary tumor, in the week leading up to re-excision and SNB.<sup>14 15</sup> Prior to routine diagnostic procedures, excised SLNs were bisected and viable cells were scraped from the cutting surface, washed, counted and further processed as previously described.<sup>15</sup> The studies were approved by the Institutional Review Board of the VU University Medical Center and written informed consent was obtained from each patient before treatment in accordance with the Declaration of Helsinki.

### Immunohistochemistry (IHC) studies

Twenty-three patients were randomly assigned to receive one preoperative intradermal injection of either 8mg CpG-B dissolved in 1.6mL of saline (NaCl 0.9%; n=11) or 1.6mL of plain saline alone (n=12) 7 days before the re-excision and SNB.<sup>12</sup> One patient, who received CpG-B, was excluded from our analyses because the patient did not undergo re-excision. The excision margin was 1cm for melanomas with a Breslow thickness of  $\leq 2$ mm and 2cm for lesions  $\geq 2$ mm. See [table 1](#) for an overview of these patients' clinical characteristics.

### Transcriptional analyses

Nineteen patients were randomly assigned to receive 4mL intradermal injections of either 1mg CpG-B (n=10) or of saline (n=9), 7 and 2 days before re-excision and SNB. Viable peripheral blood mononuclear cells (PBMCs) were isolated prior to the injections on day -7 and prior to re-excision and SNB on day 0 and cryopreserved for further transcriptional and flow cytometric analysis as previously described.<sup>16</sup>

### IHC of the skin

Paraffin sections (4 $\mu$ m) of the re-excision skin samples of 22 patients were collected, mounted on Superfrost Plus glass slides, and dried overnight at 37°C. After deparaffination, the tissue sections were hydrated through decreasing (v/v) percentages of ethanol and endogenous peroxidase was blocked with 0.1% hydrogen peroxide in methanol. Antibodies against CD1a (MTB1), CD14 (EPR3653), CD83 (1H4B/MONX10851, Monosan, Uden, The Netherlands), Langerin (12D6, Novocastra, Newcastle, UK), CD123 (7G3), DC-SIGN (DCN46, BD

**Table 1** Patient characteristics

Characteristic	Total		CpG-B		Saline	
	n	%	n	%	n	%
<i>Total</i>	22	100	10	45	12	55
Sex						
Male	14	64	6	60	8	67
Female	8	36	4	40	4	33
Age (years)						
Range	26–75		33–75		26–71	
Mean	53,22		50,86		55,19	
Site of primary melanoma						
Trunk	12	55	6	60	6	50
Upper extremity	3	14	1	10	2	17
Lower extremity	7	31	3	30	4	33
Head/Neck	0	0	0	0	0	0
Breslow thickness (mm)						
Median	1.55		1.42		1.6	
Mean	1.63		1.56		1.68	
Type of melanoma						
Superficial spreading	16	73	7	70	9	75
Nodular	4	18	1	10	3	25
Spitzoid	1	5	1	10	0	0
Acrolent	1	5	1	10	0	0
Clark level						
II	3	14	2	20	1	8
II-III	3	14	2	20	1	8
III	3	14	1	10	2	17
IV	13	59	5	50	8	67
Ulceration						
Absent	19	86	9	90	10	83
Present	3	14	1	10	2	17
Lymphatic invasion						
Absent	22	100	10	100	12	100
Present	0	0	0	0	0	0
Sentinel node						
positive	6	27	2	20	4	33
Negative	16	73	8	80	8	67
Inflamed aspect re-excision specimen						
Absent	14	64	4	40	10	83
Present	8	36	6	60	2	17
Melanoma found in re-excision specimen						
Absent	22	100	10	100	12	100
Present	0	0	0	0	0	0

Pharmingen, San Jose, USA), CD3 (F7.2.38), and CD68 (KP1, Dako, Heverlee, Belgium) were used. An IgG1 mouse-anti-human isotype control was used (MOPC 21, Organon Teknika-Cappel, Boxtel, The Netherlands).

The slides were pretreated with 10 mM TRIS, 1 mM EDTA pH 9 (CD3, CD14, CD123, DC-SIGN, CD68) or 10 mM Na-citrate pH 6 (CD1a, CD83, Langerin). Primary antibodies were applied and visualization was performed with

Bondmax (Menarini Group, Malmö, Sweden) for CD3, the Power Vision plus™ system (Immunologic, Duiven, The Netherlands) for CD14, and the Envision™ horse-radish peroxidase system (DakoCytomation, Glostrup, Denmark) for the other markers, all according to the manufacturer's instructions.

### IHC quantification

All slides were coded and counted by two independent observers blinded to the patients' treatment. The number of positive cells in the epidermis, the superficial papillary dermis (stratum papillare) and the reticular dermis (stratum reticulare) were evaluated by direct counting of stained nucleated cell bodies per ×400 magnification microscopic field, that is, high power field (HPF). Each observer counted 10 HPFs in the epidermis, the superficial dermis, defined as the HPF adjacent the epidermis, and the reticular dermis. Counts were calculated as the average of the independent observers and expressed as mean number of positive cells per HPF.

### Double or triple immunofluorescent IHC

Paraffin sections were cut (4 μm) and dried overnight on coated slides at 37°C. After deparaffination, the tissue sections were hydrated through decreasing (v/v) percentages of ethanol and incubated for 10 min in boiling antigen retrieval buffer EDTA. After cooling and washing, the slides were incubated overnight in a moist chamber with antibodies against BDCA2 (Miltenyi Biotec, Bergisch Gladbach, Germany, mouse IgG2a, 201A), CD123 (BD Pharmingen, San Jose, USA, mouse IgG2a, 7G3), CD83 (Monosan, mouse IgG1, 1H4B/MONX10851), BDCA3 (LifeSpan Biosciences, Rabbit monoclonal, LS-B7307/35332), Clec9a (R&D, Sheep IgG, AF6049). After washing, slides were incubated for 1 hour with isotype-specific secondary antibodies: GaM IgG1 (CD83) (647, blue or 546, red), GaM IgG2a (BDCA2 or CD123) (488, green), GaR (BDCA3) (546, red), Donkey anti-sheep (Clec9) (488, green). As control slides were incubated with secondary antibodies only. After washing, slides are covered with 1 drop of MOWIOL and with a coverslip and stored at 4°C. The slides were evaluated using a fluorescence microscope (Axiovert-200M) at magnifications of ×100 and ×400, and pictures were taken with a sensicam camera (PCO) and Slidebook 6 reader software (Intelligent Imaging Innovations).

### Flow cytometric analyses

DC subsets from PBMC or SLN single-cell suspensions, isolated and prepared as previously described,<sup>16 17</sup> were phenotypically analyzed by 4 or 10 color flow cytometry, with the following mAbs, which were diluted in Phosphate Buffered Saine (PBS) supplemented with 0.1% Bovine Serum Albumin (BSA) and 0.02% NaN<sub>3</sub>, and incubated for 30 min at 4°C: CD11c, CD1a, CD14, PD-L1, CD16 (BD Biosciences), CD40, CD83 (Beckman Coulter), CD86, CD80 (BD Pharmingen), BDCA3 (Miltenyi Biotec), CLEC9A, CD1c, BDCA3, CD103 (Biolegend), CD83,

PD-L1 (BD Horizon). After incubation, cells were washed in FACS buffer to remove excess antibodies and used for flow cytometric analyses. Flow cytometric analyses were performed on a FACS-Calibur flow or LSR Fortessa cytometer (Becton Dickinson), equipped with Cellquest or FACSDiva data acquisition software, respectively; data were analyzed using CellQuest (BD Biosciences) or Kaluza (Beckman Coulter) analysis software.

### PBMC cultures

PBMCs obtained from healthy donors on written informed consent (Sanquin Blood Supply Services, Amsterdam, The Netherlands) were plated in RPMI medium (BioWhittaker, Verviers, Belgium) supplemented with 10% heat inactivated fetal calf serum (Hyclone Laboratories, Logan, Utah, USA), 100 IE/mL sodium penicillin, 100 μg/mL streptomycin sulfate, 2 mM L-glutamine, and 50 μM β-mercaptoethanol (at 5 million/mL) and cultured for 48 hours in the absence or presence of 5 μg/mL CpG-B/CPG7909. After 48 hours, supernatants were collected for chemokine analysis and the cells were harvested and analyzed by flow cytometry for APC subset frequencies and activation state. Additionally, CD14<sup>+</sup> cells were isolated by magnetic activated cell sorting (MACS) by the use of CD14 magnetic beads (MACS Miltenyi Biotec), and subsequently, CD11c<sup>+</sup> cells were similarly MACS-isolated by a two-step incubation with anti-CD11c (BD Biosciences), followed by goat-anti-Mouse magnetic beads, both according to the manufacturer's protocols. The CD14<sup>+</sup> (monocytic) and CD14<sup>+</sup>CD11c<sup>+</sup> (cDC enriched) populations were plated separately (at 1 million/mL) and cultured overnight, after which supernatants were collected for chemokine analysis by flow cytometric cytokine bead array analysis according to the manufacturer's instructions (BD Biosciences).

### Type-I IFN response transcript analysis

Total RNA was isolated from PBMC and reverse transcribed as previously described.<sup>18</sup> Forty-seven type I IFN response genes (IRGs) were selected based on significant upregulation in more than three experiments published on the Interferome database (<http://www.interferome.org/>). Custom-designed TaqMan assays for each IRG were supplied by Applied Biosystems. Quantitative PCR (qPCR) analysis was performed (ServiceXS B.V., Leiden, The Netherlands) using the 96.96 BioMark Dynamic Array for real-time PCR (Fluidigm Corporation, San Francisco, California, USA), according to the manufacturer's instructions. Thermal cycling and real-time imaging of the BioMark array was carried out on the BioMark instrument, and cycle threshold (CT) values were extracted using BioMark real-time PCR analysis software. Relative quantities were calculated using the standard curve method, with glyceraldehyde-3-phosphate dehydrogenase (GAPDH) as a housekeeping gene. Expression levels were <sup>2</sup>log-transformed. An overall IRG score was determined by averaging the relative expression levels of all 47

IRG. Comparison of IRG expression between time points was assessed using paired t-tests.

### Statistical analysis

Differences in measured immune parameters between patient study groups or time points were analyzed using the two-sample Mann-Whitney U test, the Fisher's exact test, or a two-sided Student's t-test (in case of normal distribution). Correlations were determined by using Pearson r test. Microsoft Excel (V.2010) and GraphPad Prism (V.6.02) were used for all graphs, tables and analyses.  $p < 0.05$  was considered significant.

## RESULTS

### IHC analysis of APC subsets at the CpG-B-injected versus saline-injected re-excision skin site

In a two-armed randomized trial aiming at immune modulation of the SLN in early-stage melanoma, patients were treated with an intradermal injection of either 8 mg CpG-B or plain saline (placebo control group) at the primary tumor re-excision site. There were no significant differences in patient and tumor characteristics at baseline or after pathological assessment of the re-excision specimens and SLN between the two patient groups (table 1). However, routine examination of re-excision specimens by a pathologist (who was blinded to the experimental treatment arms) reported that 6 out of 10 CpG-B-injected samples had an inflamed aspect showing mononuclear immune infiltrates that could not be explained as a reaction to the suture material used after the primary melanoma excision. In contrast, in re-excision specimens of saline injected patients mostly giant cell reactions to the suture materials were reported. Of note, no melanoma cells were found in any of the 22 re-excision specimens included in this study.

IHC staining with various lineage markers revealed the frequency and distribution of various APC subsets in the skin. As shown in figure 1, in CpG-B-treated skin the epidermis and superficial or papillary dermis, immediately underlying the epidermis, showed an aspect consistent with steady state, that is, CD1a<sup>+</sup>Langerin<sup>+</sup> LCs located in the epidermis and scattered DC-SIGN<sup>+</sup> APC in the superficial dermis, without any sign of DC activation and migration (ie, lack of CD83 expression in the papillary dermis). In contrast, in the reticular dermis aggregates of CD83<sup>+</sup> and CD123<sup>+</sup> cells were observed without any evidence of colocalized DC-SIGN expression. This indicated the recruitment of DC subsets from peripheral blood, other than monocyte-derived APC, as these might be expected to express DC-SIGN. Quantification revealed no differences in APC subset markers between saline-injected or CpG-B-injected specimens in the epidermis or papillary dermis, except for a slight elevation in CD14<sup>+</sup> cells (figure 2A,B). In contrast, significantly higher numbers of CD83<sup>+</sup>, CD68<sup>+</sup>, CD123<sup>+</sup>, and CD14<sup>+</sup> cells were

found in the reticular dermis of CpG-B-injected re-excision samples as compared with saline-injected samples (figure 2C).

To further determine the identity of these APC recruited to the reticular dermis, we performed double and triple fluorescent IHC analyses on skin sections from CpG-B-administered patients (n=6). Also, two saline-injected samples were stained as negative controls. Double staining with BDCA2 (CD303) revealed the CD123<sup>+</sup> cells in CpG-B-injected skin to be pDC (in contrast, hardly any double positive pDC were observed in saline-injected samples), but double staining with CD83 revealed these pDC to be mostly immature (figure 3A). Triple staining demonstrated the CD83<sup>+</sup> cells in the reticular dermis to be mostly positive for CD141/BDCA3 and CLEC9A, identifying them as mature cDC1 (figure 3B). As a positive control, a representative example of this CD83/CD141/CLEC9A triple stain on a tonsil section is shown in online supplemental figure 1. Quantification showed a significantly higher percentage of cDC1 to be CD83<sup>+</sup> as compared with pDC (figure 3C) and that indeed the majority of CD83<sup>+</sup> cells in the reticular dermis consisted of cDC1 (70%, see figure 3D).

### Co-recruitment of cDC1 and CD14<sup>+</sup> APC to the SLN and primary tumor excision site

We previously described the preferential recruitment and activation of both CD14<sup>-</sup> and CD14<sup>+</sup> LNR-cDC/APC subsets in the melanoma SLN from CD141<sup>+</sup> and CD14<sup>+</sup> blood-derived precursors on intradermal injection of CpG-B.<sup>16</sup> This was indeed borne out by flow cytometric analyses of available cryopreserved SLN single-cell suspensions from the same patient cohort tested by IHC for APC recruitment to the CpG-B-injected or saline-injected re-excision site (figure 4A). Of note, we previously reported both CD141 and CLEC9A expressions on LNR-cDC,<sup>16</sup> identifying them as cDC1-like. Thus, the CD14<sup>-</sup> and CD14<sup>+</sup> LNR-cDC/APC subsets were strongly reminiscent of the respective cDC1 and CD14<sup>+</sup> APC subsets found to be recruited to the skin on CpG-B injection. Correlation analyses, including matched SLN and skin samples, indeed revealed co-recruitment of CD14<sup>-</sup> CD83<sup>+</sup> cDC1 and CD14<sup>+</sup> APC subsets to the SLN and skin/injection site (figure 4B).

To further ascertain their possible origins and the effects of CpG-B on these myeloid APC subsets, we performed 48-hour cultures of PBMC from healthy donors, in the presence or absence of 5 µg/mL CpG-B (CPG7909). Based on CD1c and CD141/BDCA3 expression, we distinguished three cDC subsets, and based on CD16 expression, two CD14<sup>+</sup> monocytic APC subsets post-culture. Gating strategies for these myeloid cDC and monocytic APC subsets are shown in online supplemental figure 2A. No significant differences in the distribution of these subsets between the control and CpG-B culture conditions were observed (online supplemental figure 2B). Of the three identified cDC subsets, one (CD1c<sup>+</sup>BDCA3<sup>dim</sup>) did not respond to CpG-B exposure, with only a significant

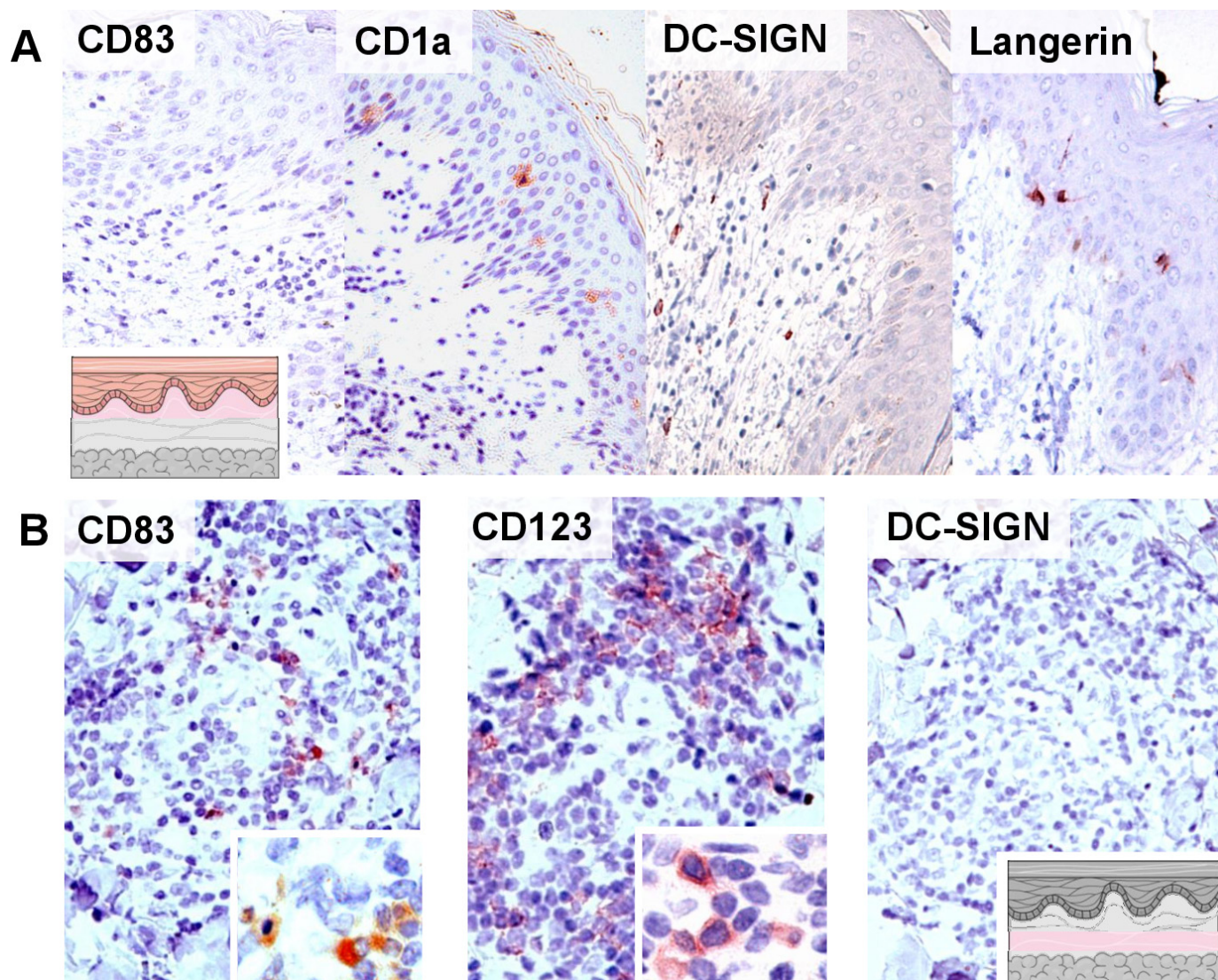


**Figure 1** Lack of activation of migratory dendritic cell subsets, but mobilization of mature and CD123<sup>+</sup> dendritic cells (DCs) to the reticular dermis in CpG-B injected primary melanoma re-excision skin specimens 7 days after injection of CpG-B. Immunohistochemical analysis of primary melanoma re-excision skin specimens 7 days after injection of CpG-B. Schematic skin representations show displayed skin sections in pink. (A) Epidermis+papillary dermis: CD1a<sup>+</sup>Langerin<sup>+</sup> Langerhans cells (LCs) were only present in the epidermis, whereas DC-SIGN<sup>+</sup> antigen-presenting cell (APC) were detected in the papillary dermis, without signs of activation or migration (lack of CD83 expression in either epidermis or dermis). (B) In the reticular dermis, CD123<sup>+</sup> APC (plasmacytoid DC) and CD83<sup>+</sup> mature dendritic cells were observed but no DC-SIGN<sup>+</sup> APC.

upregulation of CD80. In contrast, the other two subsets (ie, CD1c<sup>+</sup>BDCA3<sup>+</sup> and CD1c<sup>+</sup>BDCA3<sup>dim</sup>) both responded by significant upregulation of CD83, indicating maturation induction (figure 5). In addition, upregulation (at varying significance levels) of CD80, PD-L1, CLEC9A, and CD103 was observed. Expression (at varying levels) of CD141/BDCA3, CLEC9A, and CD103, in all three cDC subsets, identified them as cDC1-like. In contrast, no expression of CD103 or CLEC9A was observed in the CD14<sup>+</sup> APC as well as low expression levels of CD83 (the latter being marginally and non-significantly up-regulated by CpG-B) (figure 5). A remarkable upregulation of CD16 in the monocytes was observed on culture, indicative of a more inflammatory phenotype (online supplemental figure 2A). In both CD16<sup>-</sup> and CD16<sup>+</sup> monocytes,

a significant upregulation of both CD80 and PD-L1 was observed (figure 5).

Combined, our IHC data in skin, our flow cytometric data from matched SLN samples, and our in vitro culture data suggest CpG-B-induced activation of both mature cDC1 and more immature CD14<sup>+</sup> APC and their co-recruitment from PB precursors to both the skin injection site and the draining SLN.

#### T cell infiltration in relation to recruited APC subsets

IHC analyses further revealed significantly higher numbers of CD3<sup>+</sup> T cells infiltrating the papillary dermis, and even more so the reticular dermis, of CpG-B-injected skin as compared with saline-injected skin (figure 6A,B). As a growing number of studies have shown DC to be vital

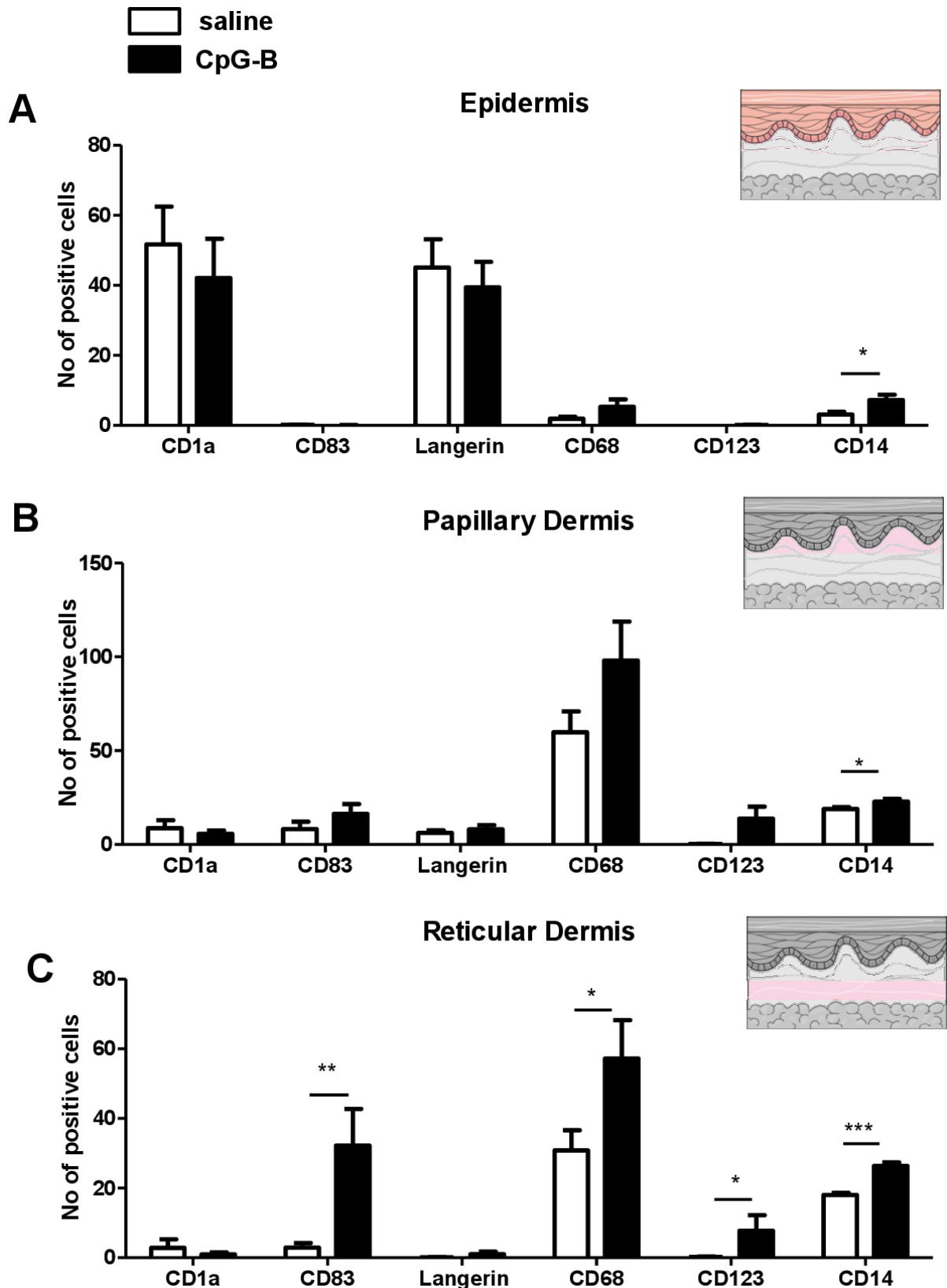


**Figure 2** Immunohistochemical quantitation reveals CpG-B-induced accumulation of mature DC and CD123<sup>+</sup>, CD14<sup>+</sup> and CD68<sup>+</sup> antigen-presenting cell (APC) in the reticular dermis of primary melanoma re-excision skin specimens. In the (A) epidermis and (B) papillary dermis, no differences except for a slight elevation in CD14<sup>+</sup> cells was found in CpG-B-injected re-excision samples (closed bars) as compared with saline-injected samples (open bars). In the (C) reticular dermis, significantly higher numbers of CD83<sup>+</sup>, CD68<sup>+</sup>, CD123<sup>+</sup>, and CD14<sup>+</sup> cells were present in CpG-B-injected re-excision samples as compared with saline-injected samples. Schematic skin representations show epidermis, papillary dermis, and reticular dermis in pink. Statistical significance: \*p<0.05; \*\*p<0.01; \*\*\*p<0.001.

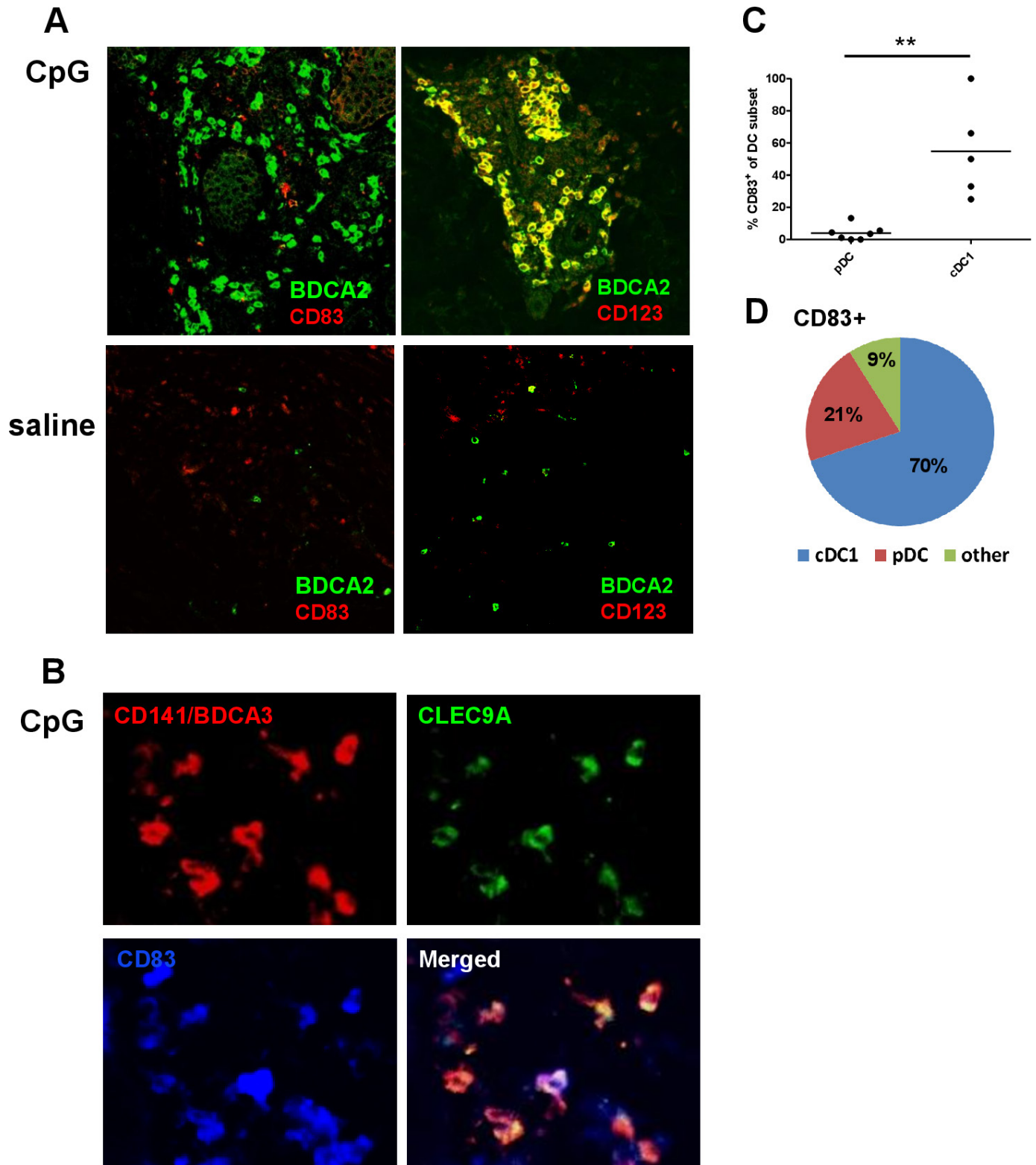


**Figure 3** Identification of CD83<sup>+</sup> cDC1 and CD83<sup>+</sup> plasmacytoid dendritic cell (pDC) in the reticular dermis. (A) Double fluorescent immunohistochemical (IHC) analyses with BDCA2 (green) and CD83 (red), and BDCA2 (green) and CD123 (red) on skin sections from CpG-B-injected and saline-injected patients revealed the presence of mainly immature pDC only in CpG-B-injected sections. (B) Triple fluorescent IHC analyses revealed that the CD83<sup>+</sup> cells (blue) in CpG-B injected sections were mostly positive for CD141/BDCA3 (red) and CLEC9A (green), identifying them as mature cDC1. Quantification showed (C) a significantly higher percentage of cDC1 to be CD83<sup>+</sup> as compared with pDC and (D) that the majority (70%) of CD83<sup>+</sup> cells were indeed cDC1 in CpG-B injected sections. Statistical significance: \*\* $p < 0.01$ .



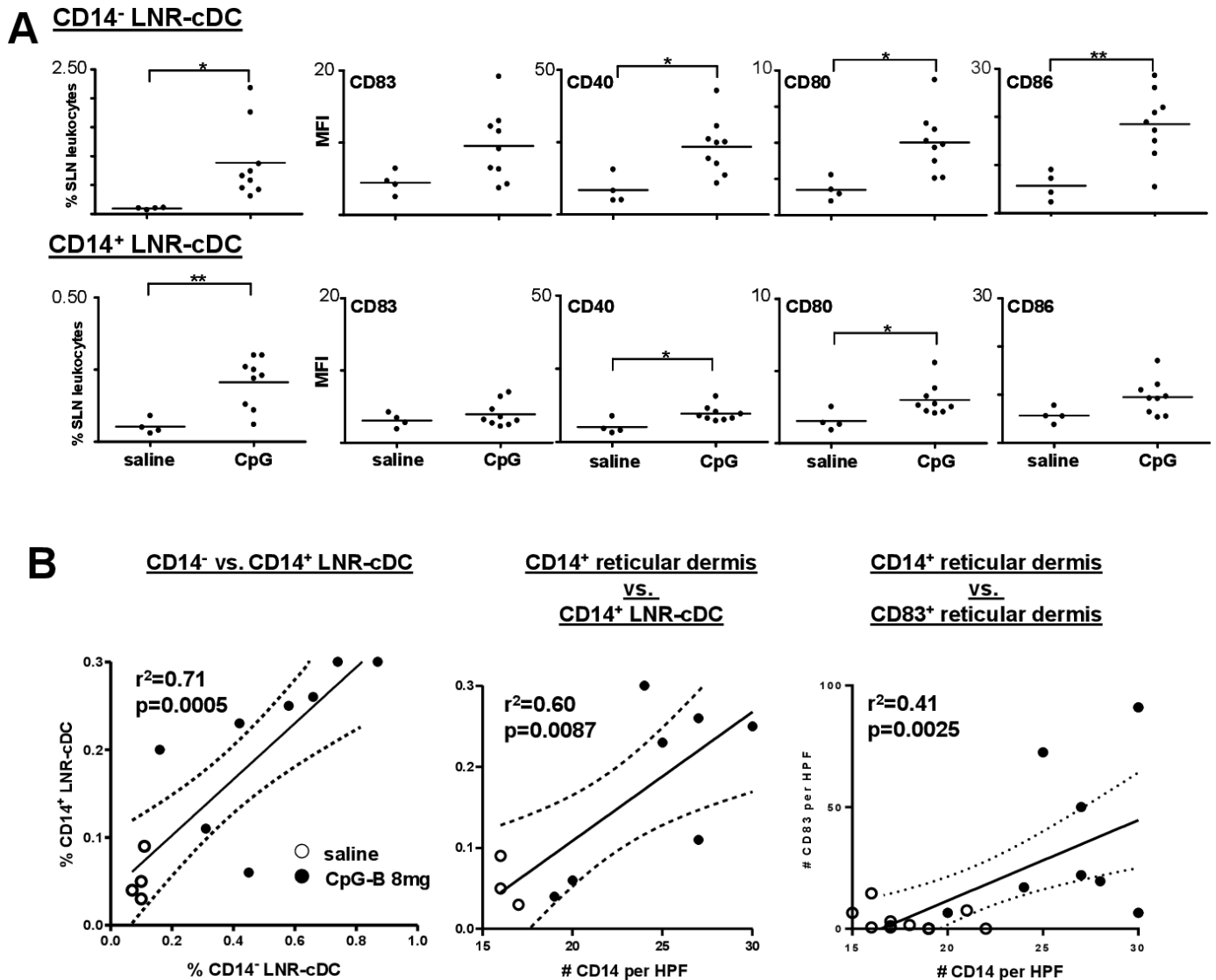


**Figure 4** Coordinated recruitment of CD14<sup>-</sup>CD83<sup>+</sup> cDC1 and CD14<sup>+</sup> antigen-presenting cell (APC) subsets to the sentinel lymph node (SLN) and reticular dermis of primary melanoma re-excision skin specimens. (A) Higher frequencies (of total SLN leukocytes) and activation states of CD14<sup>+</sup> and CD14<sup>-</sup> LNR cDC (characterized by flow cytometry for multiple markers—expressed by mean fluorescence intensity (MFI) on the specific subset) in CpG-B-treated patients and (B) correlative analyses indicate co-recruitment of CD14<sup>-</sup>CD83<sup>+</sup> cDC1 and CD14<sup>+</sup> APC subsets to the SLN and skin. Statistical significance: \* $p < 0.05$ ; \*\* $p < 0.01$ .

for the recruitment of an effector T cell infiltrate to the melanoma TME,<sup>19–22</sup> we correlated the T cell numbers to the numbers of the different APC subsets in the reticular dermis of all tested re-excision specimens. As shown in [figure 6C](#), only a weak correlation with pDC numbers was observed, but a strong and significant correlation with CD83<sup>+</sup> (cDC1) and an even stronger and more significant correlation with CD14<sup>+</sup> APC numbers was found. Indeed, whereas combined CD83 and CD14 numbers showed a strong correlation to CD3 numbers infiltrating into the reticular dermis, further inclusion of pDC numbers did not add to the strength of this correlation ([figure 6D](#)). These data suggest a dominant role for CpG-B-recruited cDC1 and CD14<sup>+</sup> APC over pDC in effecting subsequent T cell infiltration.

### CpG-B conditioned cDC1 and CD14<sup>+</sup> APC as a source of T cell attracting chemokines

To further substantiate a role for cDC1 and CD14<sup>+</sup> APC precursors recruited from blood for the subsequent mobilization of T cells, we assessed cDC1 activation and effector chemokine expression by transcriptional profiling of pretreatment and post-treatment PBMC from patients with clinical stage I/II melanoma participating in another randomized phase II clinical trial. In this trial, patients received either two intradermal injections adjacent to the primary tumor excision scar of 1 mg CpG-B/CPG7909 or of saline, 7 and 2 days prior to re-excision and SNB.

First, we showed that this treatment regimen led to a similar co-recruitment of CD14<sup>-</sup> and CD14<sup>+</sup> LNR-cDC/

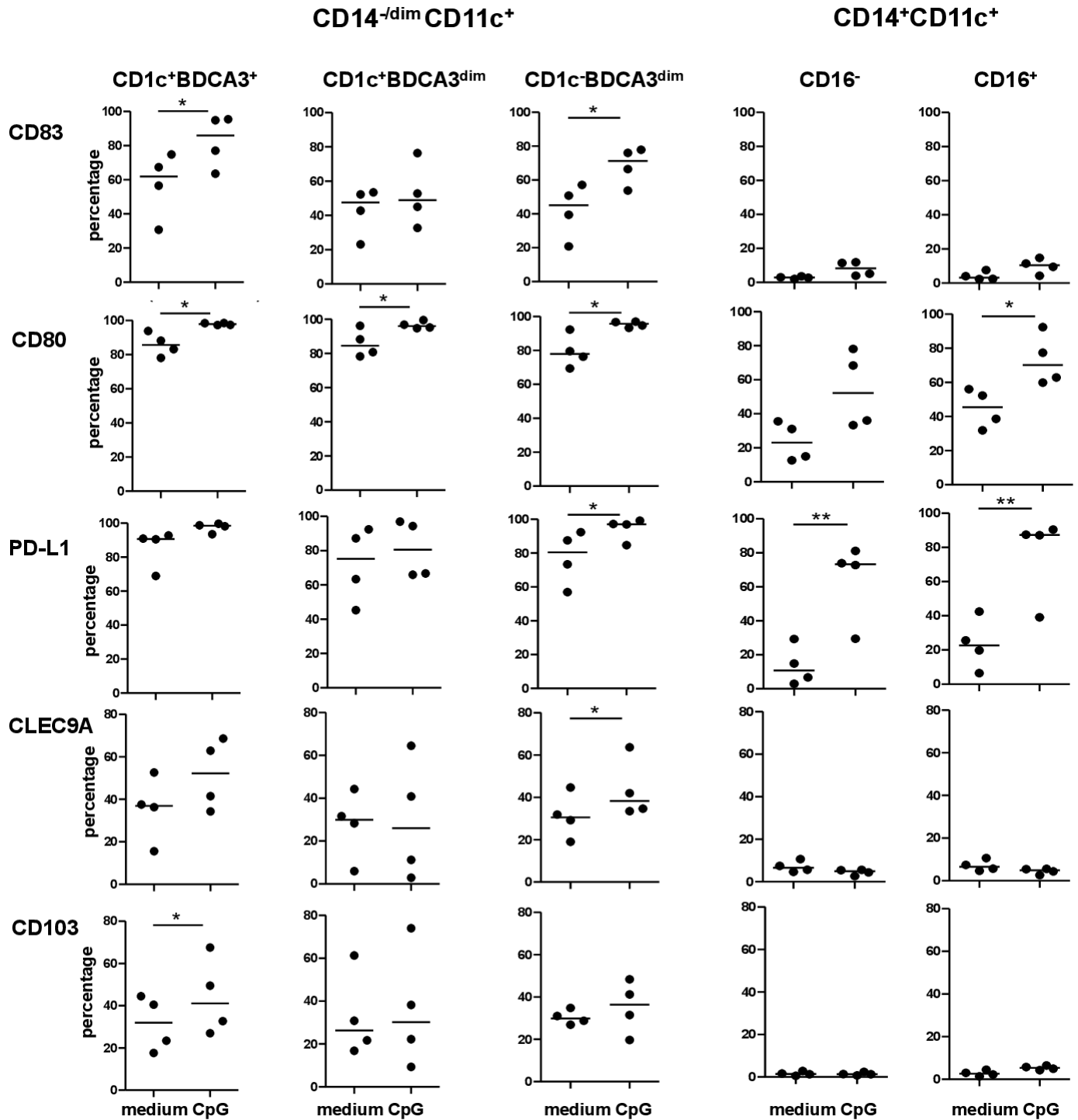


**Figure 5** In vitro activation by CpG-B of cDC1 and CD14<sup>+</sup> antigen-presenting cell (APC) subsets. Peripheral blood mononuclear cells from healthy donors (n=4) were cultured with 5 µg/mL CpG-B (CPG7909) for 2 days. CD1c<sup>+</sup>BDCA3<sup>+</sup> and CD1c<sup>-</sup>BDCA3<sup>dim</sup> subsets both responded to CpG-B by significant upregulation of CD83, indicating maturation induction. Expression of CD141/BDCA3, CLEC9A, and CD103, in all three CD14<sup>-dim</sup> subsets, identified them as cDC1-like. In contrast, no expression of CD103 or CLEC9A was observed in the CD14<sup>+</sup> subsets as well as low expression levels of CD83 and upregulation of only CD80 and PD-L1 on culture with CpG-B. Statistical significance: \*p<0.05; \*\*p<0.01.

APC to the SLN as in the previous patient cohort, used for the IHC studies, in which patients received one intradermal injection of 8 mg CpG-B or saline (see online supplemental figure 3A). Also, by transcriptional analysis of 47 known IFN-I response genes (IRG), we showed that there was a significant induction of a type-1 IFN response

measurable in PBMC, 7 days after the first intradermal injection of CpG-B (IRG scores, based on averaged relative IRG levels shown in online supplemental figure 3B). Moreover, this IRG score correlated significantly with the CD14<sup>-</sup> and CD14<sup>+</sup> LNR-cDC rates in SLN (online supplemental figure 3C), in keeping with our previous

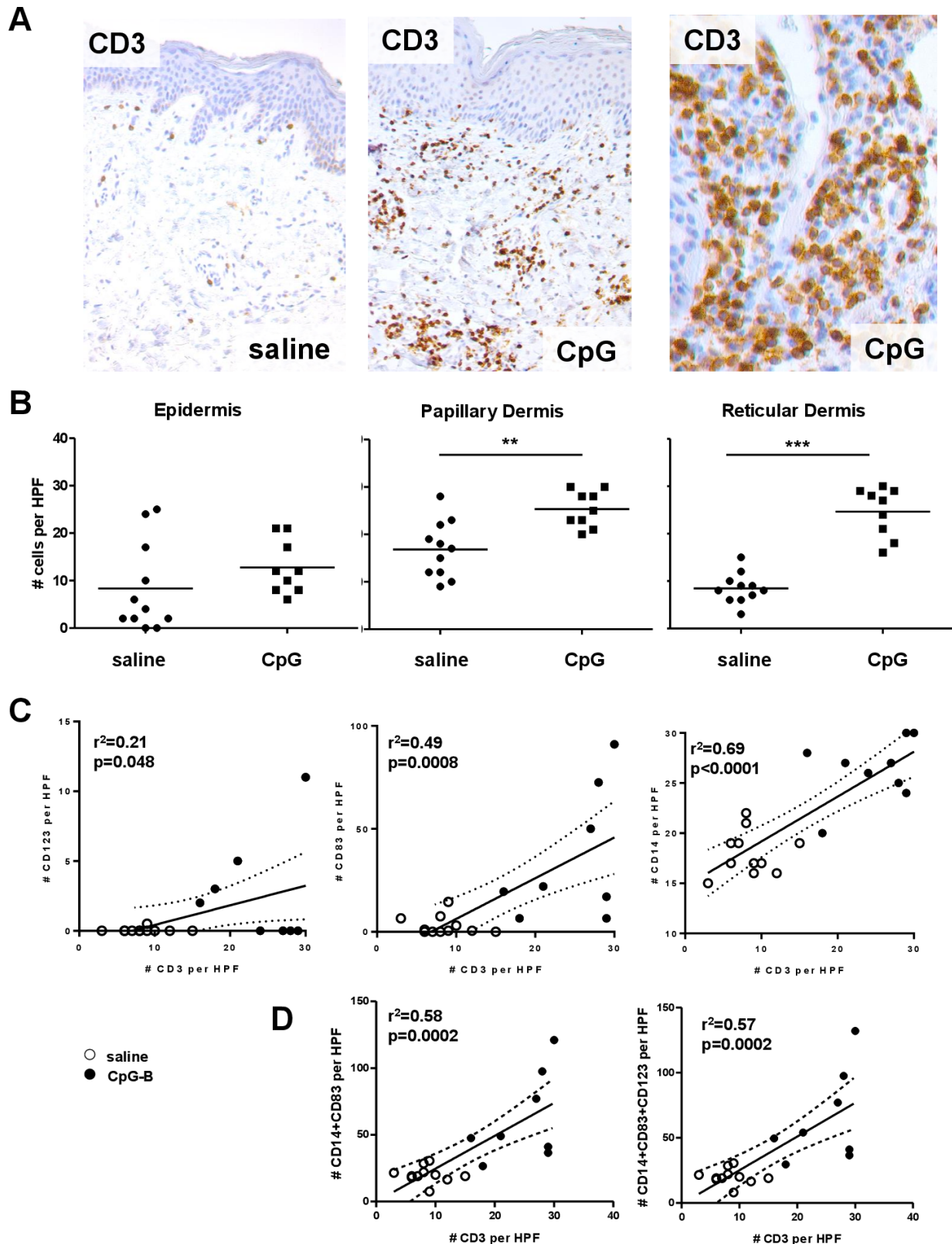


**Figure 6** Dermal T cell infiltration is related to recruited CD83<sup>+</sup> cDC1 and CD14<sup>+</sup> antigen-presenting cell (APC) subsets. (A) Immunohistochemical analyses of CD3 revealed (B) significantly higher numbers of CD3<sup>+</sup> T cells infiltrating the papillary dermis, and even more so the reticular dermis, of CpG-B-injected skin as compared with saline-injected skin. (C) Correlation of T cell numbers to the numbers of the different APC subsets in the reticular dermis of all tested re-excision specimens shows a weak correlation with plasmacytoid dendritic cell (pDC) numbers but a strong and significant correlation with CD83<sup>+</sup> (cDC1) and an even stronger and more significant correlation with CD14<sup>+</sup> APC. (D) Combined CD83 and CD14 numbers showed a strong correlation to CD3 numbers infiltrating into the reticular dermis, whereas further inclusion of pDC numbers did not add to the strength of this correlation. Statistical significance: \*\*p<0.01; \*\*\*p<0.001.

observation of a CpG-B/type-1 IFN-induced recruitment of cDC1 and CD14<sup>+</sup> APC/cDC to the SLN.<sup>16</sup>

As the IFN-inducible transcription factor IRF8 had previously been reported as vital for terminal cDC1 differentiation,<sup>23</sup> we determined its transcript levels and indeed found them to be significantly upregulated post CpG-B administration (figure 7A). Also, the known IRGs CXCL10 and CXCL11 were part of the 47 IRG signature. The transcript levels of both these effector T cell attracting chemokines were also significantly elevated after CpG-B treatment (figure 7B,C). Importantly, expression levels of all three transcripts were significantly correlated to LNR-cDC frequencies (figure 7), indicating that the CpG-B-triggered IFN-I response led to cDC1 activation in conjunction with CXCL10 and CXCL11 expressions. Online supplemental figure 3 shows a heat map of Pearson correlation p values for the IRF8 and the separate or combined CXCL10 and CXCL11 transcript levels versus the separate or combined CD14<sup>+</sup> and CD14<sup>+</sup> cDC rates in the SLN. IRF transcripts were only significantly correlated to the CD14<sup>+</sup> LNR-cDC rates, consistent with their cDC1-like state. In contrast, the chemokine transcript levels were highly significantly correlated to the frequencies of both subsets.

To confirm CpG-B-induced production of effector T cell attracting chemokines by both cDC1 and CD14<sup>+</sup> APC, we determined chemokine release levels 48 hours after in vitro PBMC exposure to CpG-B. As shown in figure 7E, this led to elevated release levels of CXCL10, CXCL9, and CXCL11, which reached significance only in the case of CXCL10. At 48 hours, CD14<sup>+</sup> and CD14<sup>+</sup>CD11c<sup>+</sup> (ie, enriched for cDC1, see online supplemental figure 2) cells were sorted from the CpG-B-exposed PBMC cultures and put in culture separately. Supernatants were collected after overnight culture and both were found to contain variable but equally high levels of CXCL10, confirming production of this effector T cell attracting chemokine by both CD14<sup>+</sup> APC and by cDC1 (figure 7F).

## DISCUSSION

In this study, we have shown that intradermal injection of CpG-B at the primary melanoma excision site results in an immune reaction in the skin that is still observed 1 week after administration (time of the re-excision).

Whereas LCs are uniquely localized in the epidermis, a complex network of varying APC subsets are found in the human dermis.<sup>1 24 25</sup> In human skin, a low-frequency dermal CD141<sup>+</sup> cDC1 subset has been described, most likely derived from CLA<sup>+</sup> bloodborne cDC1 precursors with skin homing capacity.<sup>1</sup> cDC2 subsets are more numerous. Of note, both cDC1 and cDC2 may acquire CD1a and CD1c expressions in the human dermal micro-environment.<sup>1</sup> Monocyte-derived DCs can be recruited to the dermis under inflammatory conditions but in males they are hard to discern from cDC2 as both may display varying levels of CD1 and CD14 molecules. All skin DC subsets express CCR7 on activation and can migrate

to paracortical T cell areas in draining lymph nodes. Whereas cDC1 have previously been implicated in the subsequent generation of Th1/CTL antitumor immunity, more recent insights have also revealed a clear role in this process for migratory cDC2,<sup>26</sup> and possibly cross-talk between both subsets.<sup>27</sup>

In a previous study, we found that the intradermal injection of Granulocyte/Macrophage-Colony-Stimulating Factor (GM-CSF) in patients with early-stage melanoma resulted in an accumulation of CD1a<sup>+</sup>CD83<sup>+</sup> DC in the papillary dermis, which correlated with CD1a<sup>+</sup>CD83<sup>+</sup> migratory DC rates in matching SLN.<sup>28</sup> In contrast, the injection of CpG-B did not induce migration of LC and dermal DC, which was in keeping with our previous finding that the migratory DC rates were not elevated in CpG-B-conditioned SLN.<sup>12 16</sup> Rather, various DC/APC subsets were attracted primarily to the reticular dermis.

Consistent with a previous report from Haining and colleagues, we found an accumulation of pDC in the reticular dermis on CpG-B ODN injection, which were mostly immature.<sup>29</sup> In normal steady-state skin, pDCs are very rare, but the presence of immature pDC has been reported in the skin of patients with primary melanoma.<sup>30</sup> pDC can also be recruited to the skin under inflammatory conditions as in cutaneous lupus erythematosus or psoriasis.<sup>31 32</sup> Since both patient groups underwent a primary melanoma excision, often many weeks before the experimental treatment and re-excision, it is very likely that the skin at the primary excision site returned to steady state. This is in line with our finding of nearly absent pDC in the dermis of patients in the saline control group. We previously described significantly higher activation and maturation states of pDC (by CD83, CD86 and CD40) in SLN of these same patients, most likely as a result of direct TLR9 stimulation with CpG-B.<sup>12</sup> In our re-excision specimens, however, we did not find CD83 coexpression on pDC. We hypothesize that the accumulation of these immature pDCs in the re-excision specimens of patients that were treated with CpG-B is likely mediated by chemerin. Chemerin is a chemoattractant for cells that express CMKLR1 (chemokine-like receptor 1) which include circulating immature pDC (but not cDC)<sup>33</sup> and macrophages.<sup>34</sup> Chemerin is expressed as an inactive propeptide in endothelial cells and fibroblasts in the healthy skin but can be activated on skin injury<sup>35</sup> and bacterial infection<sup>36</sup> resulting in the accumulation of, among others, immature pDC (BDCA2<sup>+</sup>CD123<sup>+</sup>) and macrophages (CD68<sup>+</sup>), as we have found in the skin of the CpG-B-treated patients in our study. Remarkably, we previously did not find any increases in pDC rates in the SLN on CpG-B delivery,<sup>12 16</sup> further supporting the notion of a selective role for a skin-restricted pDC chemoattractant, like chemerin. Of note, the local increase of pDC at the injection site provides a good rationale for repeated CpG-B administrations as their effects may be further amplified by direct activation and subsequent IFN-I release on repeated CpG-B administration.

We found that the higher numbers of CD83<sup>+</sup> cells that were observed in the reticular dermis of patients who

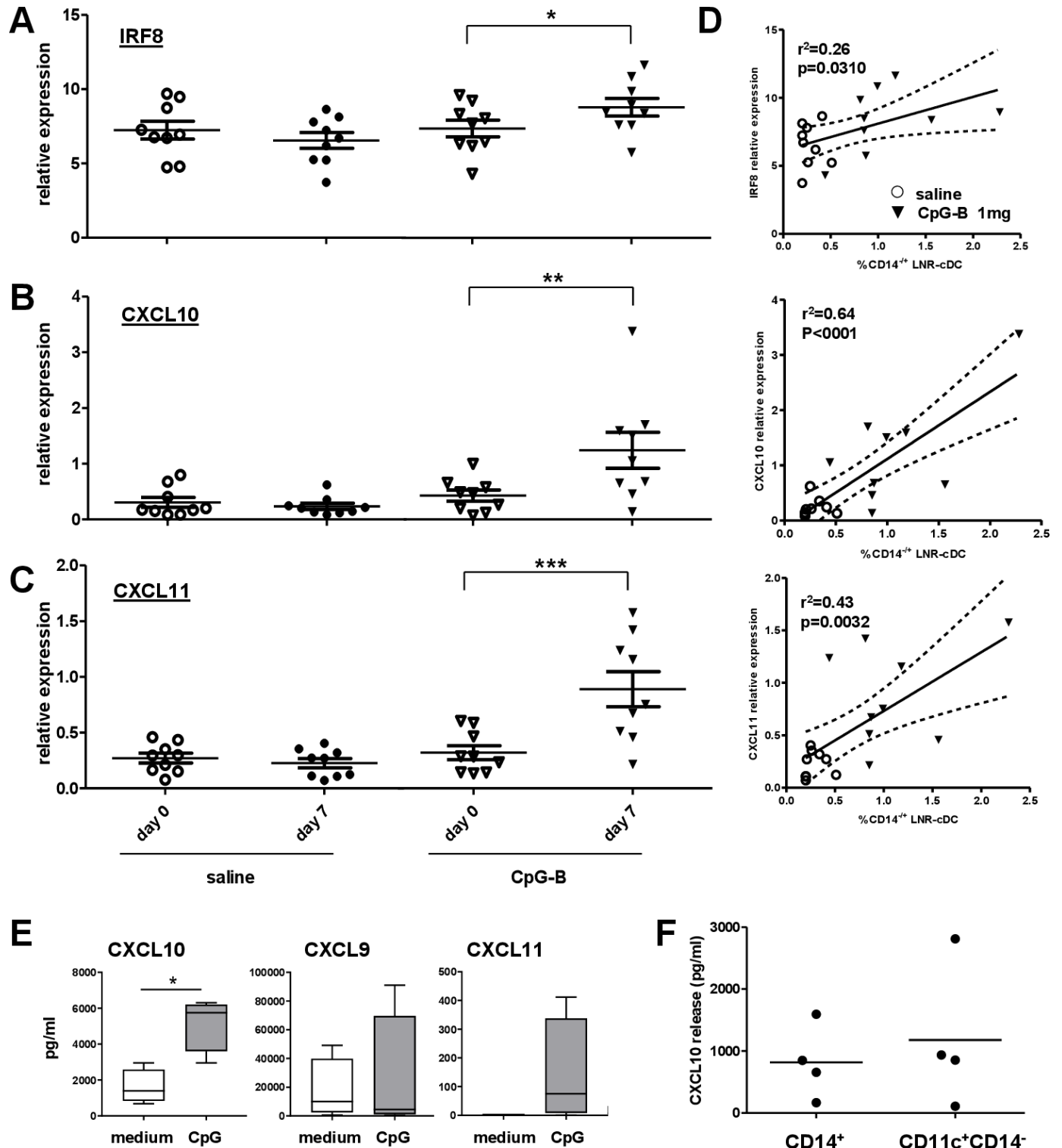


**Figure 7** Transcriptional analysis supports the relationship between CpG-B-induced cDC1 activation and recruitment and the expression of effector T cell-attracting chemokines. Significantly upregulated transcript levels of (A) IRF8, (B) CXCL10 and (C) CXCL11 were observed in peripheral blood mononuclear cell (PBMC) from patients, 7 days post local CpG-B administration as compared with pretreatment levels. (D) Expression levels of all three transcripts were significantly correlated to lymph node resident (LNR)-cDC frequencies. (E) Chemokine release assays of PBMC from healthy donors showed significantly elevated CXCL10 levels after 24 hours in vitro culture of PBMCs with CpG-B (5  $\mu$ g/mL; n=4). (F) At 48 hours, CD14<sup>+</sup> and CD14<sup>-</sup>CD11c<sup>+</sup> (ie, enriched for cDC1 cells) fractions were sorted from the CpG-B PBMC cultures and put in culture separately. Supernatants were collected after overnight culture and both were found to contain equally high levels of CXCL10. Statistical significance: \* $p<0.05$ ; \*\* $p<0.01$ ; \*\*\* $p<0.001$ .

were injected with CpG-B were not pDC but CLEC9A expressing CD141<sup>+</sup> DC. These so-called cDC1 have been recognized as powerful (cross-)primers of cytotoxic T lymphocytes (CTLs). CD141<sup>+</sup> cDC1 are known to express relatively high levels of CD83 and to originate from CD141<sup>+</sup> blood cDC1 that can be recruited to effector sites like the SLN and the skin in an IFN $\alpha$ -dependent manner, as we previously described in patients who were treated with CpG-B with or without GM-CSF.<sup>16</sup> In mouse models, endogenous type-1 IFNs also induced the accumulation of CD8 $\alpha$ <sup>+</sup> cDC1 (the murine equivalent of human CD141<sup>+</sup> cDC1) which was shown to be essential for spontaneous CTL priming against tumor antigens.<sup>37</sup> cDC1 can be attracted by the chemokines CCL5 and XCL1, which are mainly derived from NK cells,  $\gamma\delta$ T cells, or CD8<sup>+</sup> T cells, all of which are activated by type-1 IFN.<sup>38–41</sup> Of note, type-1 IFN can also induce STAT-dependent CCL5 release by keratinocytes.<sup>42</sup> cDC1 in the TME and vaccine injection sites have been shown to migrate to draining lymph nodes and to induce CTL responses there.<sup>43,44</sup> Moreover, more recent studies have demonstrated the importance of CD103<sup>+</sup> cDC1 in the release of CXCL10/CXCL9 and the subsequent attraction of effector T cells to the melanoma TME.<sup>20,21</sup> These previous observations from mostly murine studies are in keeping with our current findings from clinical specimens, showing clear correlations between CpG-induced IFN-I responses, cDC1 activation and recruitment to skin and SLN, CXCL10 expression, and T cell infiltration rates.

Besides cDC1, we also observed a significant increase in CD14<sup>+</sup> cell numbers in the CpG-B-injected skin, similar to what we previously described in lymph nodes, where CD14<sup>+</sup> and CD141<sup>+</sup> LNR-cDC were found to be present in higher numbers and activation states on CpG-B treatment.<sup>14</sup> We designated the CD14<sup>+</sup> APC in the SLN as LNR-cDC, rather than macrophages, based on their (low) expression levels of CD83 and their ability to prime allogeneic T cells.<sup>2</sup> Although we were unable to demonstrate this for the CD14<sup>+</sup> APC in the re-excision specimens, we did find that the frequencies of CD14<sup>+</sup> LNR-cDC positively correlated with the number of CD14<sup>+</sup> APC in the reticular dermis, suggestive of co-recruitment on intradermal CpG-B delivery. Flow cytometric analysis on in vitro exposure to CpG-B showed activated monocytes to acquire an inflammatory CD16<sup>+</sup> phenotype with low levels of CD83 and elevated high levels of CD80 and PD-L1, suggestive of their T cell-activating capacity. Whereas in SLN we found the CD14<sup>+</sup> APC to express CLEC9A, in the PBMC cultures we found them to be devoid of CLEC9A, which was consistent with our IHC findings in the skin re-excision samples, where CLEC9A was found to be coexpressed with CD141 and CD83, consistent with a mature cDC1 phenotype. This also is consistent with our findings in the PBMC cultures, showing CpG-B-induced elevation of levels of co-expressed CLEC9A, CD103, and CD83 on CD141<sup>+</sup> cDC1.

We previously showed a similar type-1 IFN response-related co-recruitment of cDC1 and monocytes from

peripheral blood to melanoma SLN on local delivery of CpG-B.<sup>16</sup> Both APC subsets are known to be type-1 IFN responsive, with cDC1 being activated (with increased cross-presenting ability) and classical monocytes acquiring a cDC1-like phenotype with cross-presenting abilities on IFN-1 stimulation (particularly when combined with GM-CSF).<sup>16, 45–48</sup> Subsequent locoregional recruitment of both APC subsets could have been mediated by XCL1 and CCL5, respectively.

Whereas a previous study also identified CD123<sup>+</sup> pDC surrounded by T cells in the dermis of CpG-injected vaccination sites and demonstrated an ability of pDC to attract T cells in vitro, our findings clearly suggest that the cDC1 and CD14<sup>+</sup> APC infiltrate in the reticular dermis is more vital to the subsequent recruitment of T cells. Indeed, we have observed high T cell infiltration rates on intradermal administration of CpG-B in reticular dermis that was entirely devoid of pDC (see figure 6C, left panel). Transcriptional data and data from in vitro cultures indicate an important role for CXCL10 in this regard, with CXCL10 production confirmed in vitro for both CD14<sup>+</sup> APC and cDC1.

Altogether these findings lead us to propose a model as presented in online supplemental figure 4. Intradermal injection of CpG-B triggers pDC activation and IFN-I release in the draining LN, which induces activation and subsequent recruitment of bloodborne cDC1 and monocytic precursors, both to the SLN and the skin injection site (online supplemental figure 4A). pDC attraction to the skin, but not to the SLN, may be related to dermal stroma-derived chemoattractants, such as chemerin. Of note, it is conceivable that such chemoattractants, locally induced by the direct activity of CpG-B, may be responsible for the initial recruitment of relatively small numbers of pDC and CD14<sup>+</sup> APC, which may then trigger the subsequent recruitment of more numerous cDC1/CD14<sup>+</sup> APC and T cells. Mature cDC1 from the reticular dermis may migrate to the SLN, carrying tumor-associated antigens, and may, in concert with CD14<sup>+</sup> and CD14<sup>+</sup> LNR-cDC, prime and/or boost melanoma-specific effector T cells, which, on recirculation through the blood, are attracted to effector sites (including the CpG-B injection site) by CXCL10, released predominantly by locally recruited cDC1 and CD14<sup>+</sup> APC (online supplemental figure 4B).

As a T cell-inflamed microenvironment was shown to be beneficial in the context of melanoma vaccines and immune checkpoint inhibitors,<sup>49, 50</sup> we deem intradermal or intratumoral delivery of CpG ODN an important adjuvant therapy option in support of other immunotherapy approaches. While earlier murine studies delivered proof of this concept,<sup>51, 52</sup> a recent study from Ribas and colleagues on the combination of intratumoral CpG administration and systemic PD-1 blockade confirmed this notion clinically.<sup>53</sup> Our own findings in early-stage melanoma further indicate the clinical efficacy of CpG ODN as monotherapy, locally delivered at the primary tumor excision scar, in clinical stage I-II, in a bid to overcome early LNR-cDC

suppression in the draining lymph nodes.<sup>14</sup> Indeed, Liang and colleagues showed that CpG can help overcome melanoma-related and  $\beta$ -catenin-mediated suppression of DC.<sup>52</sup> It is important to note that the study presented here carried some inherent limitations, that is, the limited numbers of available samples and the incorporation of samples and data derived from two separate phase II trials, testing different dose levels of CpG-B/CPG7909. Nevertheless, our findings from human studies are unique and shed light on events following local CpG-B delivery, which lead to locoregional recruitment of APC subsets and T cell infiltration. Locally delivered CpG ODN can thus contribute to the enhanced efficacy of systemic anti-tumor T cell responses, both in the induction and the effector phase.

#### Author affiliations

<sup>1</sup>Department of Medical Oncology, Amsterdam University Medical Centers, Vrije Universiteit, Cancer Center Amsterdam, Amsterdam, The Netherlands

<sup>2</sup>Department of Pathology, Amsterdam University Medical Centers, Vrije Universiteit, Cancer Center Amsterdam, Amsterdam, The Netherlands

<sup>3</sup>Department of Surgical Oncology, Amsterdam University Medical Centers, Vrije Universiteit, Cancer Center Amsterdam, Amsterdam, The Netherlands

<sup>4</sup>Center for Gynecological Oncology Amsterdam (CGOA), Amsterdam University Medical Centers, Vrije Universiteit, Cancer Center Amsterdam, Amsterdam, The Netherlands

**Acknowledgements** The authors would like to thank Dr Joost Oudejans for pathology assessments, Dr Art Krieg (Coley Pharmaceutical Group) for kind provision of CPG7909, and Pepijn G.J.T.B. Wijnands for excellent technical assistance. This study was supported by the Fritz Ahlqvist Foundation.

**Contributors** BDK and MLG designed and performed the research, analyzed and interpreted the data, and wrote the manuscript. MFCMvdH and AWT performed the research and collected and analyzed the data. BJRS and BGM performed the research and collected and analyzed the data. PAMvL designed the research. SV performed the research and collected and analyzed the data. RJS and AJMvdE designed the research. MPvdt collected the materials and designed the research. ESJ performed the research and collected and analyzed the data. TddG designed the research, analyzed and interpreted data, and wrote the manuscript.

**Funding** The authors have not declared a specific grant for this research from any funding agency in the public, commercial or not-for-profit sectors.

**Competing interests** No, there are no competing interests.

**Patient consent for publication** Not required.

**Provenance and peer review** Not commissioned; externally peer reviewed.

**Data availability statement** Data are available upon reasonable request. All data relevant to the study are included in the article or uploaded as supplementary information. Datasets used and analyzed during the current study are available from the corresponding author upon reasonable request.

**Supplemental material** This content has been supplied by the author(s). It has not been vetted by BMJ Publishing Group Limited (BMJ) and may not have been peer-reviewed. Any opinions or recommendations discussed are solely those of the author(s) and are not endorsed by BMJ. BMJ disclaims all liability and responsibility arising from any reliance placed on the content. Where the content includes any translated material, BMJ does not warrant the accuracy and reliability of the translations (including but not limited to local regulations, clinical guidelines, terminology, drug names and drug dosages), and is not responsible for any error and/or omissions arising from translation and adaptation or otherwise.

**Open access** This is an open access article distributed in accordance with the Creative Commons Attribution Non Commercial (CC BY-NC 4.0) license, which permits others to distribute, remix, adapt, build upon this work non-commercially, and license their derivative works on different terms, provided the original work is properly cited, appropriate credit is given, any changes made indicated, and the use is non-commercial. See <http://creativecommons.org/licenses/by-nc/4.0/>.

#### ORCID iD

Marta López González <http://orcid.org/0000-0002-8566-2200>

#### REFERENCES

- Kashem SW, Haniffa M, Kaplan DH. Antigen-Presenting cells in the skin. *Annu Rev Immunol* 2017;35:469–99.
- van de Ven R, Lindenberg JJ, Oosterhoff D, et al. Dendritic cell plasticity in tumor-conditioned skin: CD14+ cells at the cross-roads of immune activation and suppression. *Front Immunol* 2013;4:403.
- Haniffa M, Shin A, Bigley V, et al. Human tissues contain CD141hi Cross-Presenting dendritic cells with functional homology to mouse CD103+ nonlymphoid dendritic cells. *Immunity* 2012;37:60–73.
- McGovern N, Schlitzer A, Gunawan M, et al. Human dermal CD14+ cells are a transient population of monocyte-derived macrophages. *Immunity* 2014;41:465–77.
- Wollenberg A, Günther S, Moderer M, et al. Plasmacytoid dendritic cells: a new cutaneous dendritic cell subset with distinct role in inflammatory skin diseases. *J Invest Dermatol* 2002;119:1096–102.
- Moseman EA, Liang X, Dawson AJ, et al. Human Plasmacytoid Dendritic Cells Activated by CpG Oligodeoxynucleotides Induce the Generation of CD4+ CD25+ Regulatory T Cells. *J Immunol* 2004;173:4433–42.
- Munn DH, Mellor AL. The tumor-draining lymph node as an immune-privileged site. *Immunol Rev* 2006;213:146–58.
- van den Hout MFCM, Koster BD, Sluijter BJR, et al. Melanoma sequentially suppresses different DC subsets in the sentinel lymph node, affecting disease spread and recurrence. *Cancer Immunol Res* 2017;5:969–77.
- Krug A, Towarowski A, Britsch S, et al. Toll-Like receptor expression reveals CpG DNA as a unique microbial stimulus for plasmacytoid dendritic cells which synergizes with CD40 ligand to induce high amounts of IL-12. *Eur J Immunol* 2001;31:3026–37.
- Krieg AM. Cpg motifs in bacterial DNA and their immune effects. *Annu Rev Immunol* 2002;20:709–60.
- Rothenfusser S, Tuma E, Endres S, et al. Plasmacytoid dendritic cells: the key to CpG. *Hum Immunol* 2002;63:1111–9.
- Molenkamp BG, van Leeuwen PAM, Meijer S, et al. Intradermal CpG-B activates both plasmacytoid and myeloid dendritic cells in the sentinel lymph node of melanoma patients. *Clin Cancer Res* 2007;13:2961–9.
- Molenkamp BG, Sluijter BJR, van Leeuwen PAM, et al. Local Administration of PF-3512676 CpG-B Instigates Tumor-Specific CD8+ T-Cell Reactivity in Melanoma Patients. *Clin Cancer Res* 2008;14:4532–42.
- Koster BD, van den Hout MFCM, Sluijter BJR, et al. Local adjuvant treatment with low-dose CpG-B offers durable protection against disease recurrence in clinical stage I–II melanoma: data from two randomized phase II trials. *Clinical Cancer Research* 2017;23:5679–86.
- Vuylsteke RJCLM, Molenkamp BG, Gietema HA, et al. Local administration of granulocyte/macrophage colony-stimulating factor increases the number and activation state of dendritic cells in the sentinel lymph node of early-stage melanoma. *Cancer Res* 2004;64:8456–60.
- Sluijter BJR, van den Hout MFCM, Koster BD, et al. Arming the Melanoma Sentinel Lymph Node through Local Administration of CpG-B and GM-CSF: Recruitment and Activation of BDCA3/CD141+ Dendritic Cells and Enhanced Cross-Presentation. *Cancer Immunol Res* 2015;3:495–505.
- van de Ven R, van den Hout MFCM, Lindenberg JJ, et al. Characterization of four conventional dendritic cell subsets in human skin-draining lymph nodes in relation to T-cell activation. *Blood* 2011;118:2502–10.
- Koster BD, de Jong TD, van den Hout MFCM, et al. In the mix: the potential benefits of adding GM-CSF to CpG-B in the local treatment of patients with early-stage melanoma. *Oncoimmunology* 2020;9:1708066.
- Pfirschke C, Siwicki M, Liao H-W, et al. Tumor microenvironment: no effector T cells without dendritic cells. *Cancer Cell* 2017;31:614–5.
- Spranger S, Dai D, Horton B, et al. Tumor-Residing Batf3 dendritic cells are required for effector T cell trafficking and adoptive T cell therapy. *Cancer Cell* 2017;31:711–23.
- Chow MT, Ozga AJ, Servis RL, et al. Intratumoral activity of the CXCR3 chemokine system is required for the efficacy of anti-PD-1 therapy. *Immunity* 2019;50:1498–512.
- Broz ML, Binnwies M, Boldajipour B, et al. Dissecting the tumor myeloid compartment reveals rare activating antigen-presenting cells critical for T cell immunity. *Cancer Cell* 2014;26:638–52.

- 23 Sichien D, Scott CL, Martens L, *et al.* Irf8 transcription factor controls survival and function of terminally differentiated conventional and plasmacytoid dendritic cells, respectively. *Immunity* 2016;45:626–40.
- 24 Xue D, Tabib T, Morse C, *et al.* Transcriptome landscape of myeloid cells in human skin reveals diversity, rare populations and putative DC progenitors. *J Dermatol Sci* 2020;97:41–9.
- 25 Alcántara-Hernández M, Leylek R, Wagar LE, *et al.* High-Dimensional phenotypic mapping of human dendritic cells reveals interindividual variation and tissue specialization. *Immunity* 2017;47:1037–50.
- 26 Binnewies M, Mujal AM, Pollack JL, *et al.* Unleashing type-2 dendritic cells to drive protective antitumor CD4+ T cell immunity. *Cell* 2019;177:556–71.
- 27 Borst J, Ahrends T, Bąbala N, *et al.* CD4+ T cell help in cancer immunology and immunotherapy. *Nat Rev Immunol* 2018;18:635–47.
- 28 Molenkamp BG, Vuylsteke RJCLM, van Leeuwen PAM, *et al.* Matched skin and sentinel lymph node samples of melanoma patients reveal exclusive migration of mature dendritic cells. *Am J Pathol* 2005;167:1301–7.
- 29 Haining WN, Davies J, Kanzler H, *et al.* CpG oligodeoxynucleotides alter lymphocyte and dendritic cell trafficking in humans. *Clin Cancer Res* 2008;14:5626–34.
- 30 Vermi W, Bonecchi R, Facchetti F, *et al.* Recruitment of immature plasmacytoid dendritic cells (plasmacytoid monocytes) and myeloid dendritic cells in primary cutaneous melanomas. *J Pathol* 2003;200:255–68.
- 31 Farkas L, Beiske K, Lund-Johansen F, *et al.* Plasmacytoid dendritic cells (natural interferon- alpha/beta-producing cells) accumulate in cutaneous lupus erythematosus lesions. *Am J Pathol* 2001;159:237–43.
- 32 Nestle FO, Conrad C, Tun-Kyi A, *et al.* Plasmacytoid predendritic cells initiate psoriasis through interferon- $\alpha$  production. *J Exp Med* 2005;202:135–43.
- 33 Zabel BA, Silverio AM, Butcher EC. Chemokine-Like receptor 1 expression and chemerin-directed chemotaxis distinguish plasmacytoid from myeloid dendritic cells in human blood. *J Immunol* 2005;174:244–51.
- 34 Zabel BA, Ohyama T, Zuniga L, *et al.* Chemokine-like receptor 1 expression by macrophages in vivo: regulation by TGF- $\beta$  and TLR ligands. *Exp Hematol* 2006;34:1106–14.
- 35 Gregorio J, Meller S, Conrad C, *et al.* Plasmacytoid dendritic cells sense skin injury and promote wound healing through type I interferons. *J Exp Med* 2010;207:2921–30.
- 36 Kulig P, Zabel BA, Dubin G, *et al.* *Staphylococcus aureus* -derived staphopain B, a potent cysteine protease activator of plasma chemerin. *J Immunol* 2007;178:3713–20.
- 37 Fuertes MB, Kacha AK, Kline J, *et al.* Host type I IFN signals are required for antitumor CD8+ T cell responses through CD8 $\alpha$ + dendritic cells. *J Exp Med* 2011;208:2005–16.
- 38 Matsuo K, Kitahata K, Kawabata F, *et al.* A highly active form of XCL1/Lymphotactin functions as an effective adjuvant to recruit Cross-Presenting dendritic cells for induction of effector and memory CD8+ T cells. *Front Immunol* 2018;9:2775.
- 39 Böttcher JP, Bonavita E, Chakravarty P, *et al.* Nk cells stimulate recruitment of cdc1 into the tumor microenvironment promoting cancer immune control. *Cell* 2018;172:1022–37.
- 40 de Andrade LF, Lu Y, Luoma A, *et al.* Discovery of specialized NK cell populations infiltrating human melanoma metastases. *JCI Insight* 2019;4.
- 41 Rezende RM, Nakagaki BN, Moreira TG, *et al.*  $\gamma\delta$  T Cell-Secreted XCL1 Mediates Anti-CD3-Induced Oral Tolerance. *J.I.* 2019;203:2621–9.
- 42 Johansen C, Rittig AH, Mose M, *et al.* Stat2 is involved in the pathogenesis of psoriasis by promoting CXCL11 and CCL5 production by keratinocytes. *PLoS One* 2017;12:e0176994.
- 43 Bąbala N, Bovens A, de Vries E, *et al.* Subcellular Localization of Antigen in Keratinocytes Dictates Delivery of CD4+ T-cell Help for the CTL Response upon Therapeutic DNA Vaccination into the Skin. *Cancer Immunol Res* 2018;6:835–47.
- 44 Roberts EW, Broz ML, Binnewies M, *et al.* Critical role for CD103 + /CD141 + dendritic cells bearing CCR7 for tumor antigen trafficking and priming of T cell immunity in melanoma. *Cancer Cell* 2016;30:324–36.
- 45 Lapenta C, Santini SM, Spada M, *et al.* IFN- $\alpha$ -conditioned dendritic cells are highly efficient in inducing cross-priming CD8+ T cells against exogenous viral antigens. *Eur J Immunol* 2006;36:2046–60.
- 46 Lapenta C, Gabriele L, Santini SM. IFN-Alpha-Mediated differentiation of dendritic cells for cancer immunotherapy: advances and perspectives. *Vaccines* 2020;8:617.
- 47 Han S, Zhuang H, Lee PY, *et al.* Differential responsiveness of monocyte and macrophage subsets to interferon. *Arthritis Rheumatol* 2020;72:100–13.
- 48 Ruben JM, Bontkes HJ, Westers TM, *et al.* Differential capacity of human interleukin-4 and interferon- $\alpha$  monocyte-derived dendritic cells for cross-presentation of free versus cell-associated antigen. *Cancer Immunol Immunother* 2015;64:1419–27.
- 49 Ji R-R, Chasalow SD, Wang L, *et al.* An immune-active tumor microenvironment favors clinical response to ipilimumab. *Cancer Immunol Immunother* 2012;61:1019–31.
- 50 Gajewski TF, Louahed J, Brichard VG. Gene signature in melanoma associated with clinical activity: a potential clue to unlock cancer immunotherapy. *Cancer J* 2010;16:399–403.
- 51 Reilley MJ, Morrow B, Ager CR, *et al.* Tlr9 activation cooperates with T cell checkpoint blockade to regress poorly immunogenic melanoma. *J Immunother Cancer* 2019;7:323.
- 52 Liang X, Fu C, Cui W, *et al.*  $\beta$ -catenin mediates tumor-induced immunosuppression by inhibiting cross-priming of CD8+ T cells. *J Leukoc Biol* 2014;95:179–90.
- 53 Ribas A, Medina T, Kummar S, *et al.* SD-101 in combination with pembrolizumab in advanced melanoma: results of a phase Ib, multicenter study. *Cancer Discov* 2018;8:1250–7.